The Journal of Chemical Physics

Theoretical study of active secondary transport: Unexpected differences in molecular mechanisms for antiporters and symporters

Cite as: J. Chem. Phys. **156**, 085102 (2022); https://doi.org/10.1063/5.0082589
Submitted: 16 December 2021 • Accepted: 04 February 2022 • Accepted Manuscript Online: 04 February 2022 • Published Online: 22 February 2022

Alex Berlaga and Anatoly B. Kolomeisky

COLLECTIONS

This paper was selected as Featured

View Online Export Citation CrossMark

ARTICLES YOU MAY BE INTERESTED IN

A bottom-up perspective on photodynamics and photoprotection in light-harvesting complexes using anti-Brownian trapping
The Journal of Chemical Physics **156**, 070901 (2022); https://doi.org/10.1063/5.0079042

Nonequilibrium free energy during polymer chain growth
The Journal of Chemical Physics **156**, 084902 (2022); https://doi.org/10.1063/5.0080786

Modeling of biomolecular machines in non-equilibrium steady states
The Journal of Chemical Physics **155**, 230901 (2021); https://doi.org/10.1063/5.0070922

© 2022 Author(s).

The Journal of Chemical Physics ARTICLE scitation.org/journal/jcp

Theoretical study of active secondary transport: Unexpected differences in molecular mechanisms for antiporters and symporters

Cite as: J. Chem. Phys. 156, 085102 (2022); doi: 10.1063/5.0082589
Submitted: 16 December 2021 • Accepted: 4 February 2022 •
Published Online: 22 February 2022

View Online Export Citation CrossMark

Alex Berlaga[1,a] and Anatoly B. Kolomeisky[2,b]

AFFILIATIONS

[1] Department of Chemistry, Rice University, Houston, Texas 77005, USA
[2] Department of Chemistry and Center for Theoretical Biological Physics, Rice University, Houston, Texas 77005, USA

[a] Electronic mail: awb4@rice.edu
[b] Author to whom correspondence should be addressed: tolya@rice.edu. Also at: Department of Chemical and Biomolecular Engineering, Rice University, Houston, Texas 77005, USA and Department of Physics and Astronomy, Rice University, Houston, Texas 77005, USA.

ABSTRACT

Successful functioning of biological cells relies on efficient translocation of different materials across cellular membranes. An important part of this transportation system is membrane channels that are known as antiporters and symporters. They exploit the energy stored as a trans-membrane gradient of one type of molecules to transport the other types of molecules against their gradients. For symporters, the directions of both fluxes for driving and driven species coincide, while for antiporters, the fluxes move in opposite directions. There are surprising experimental observations that despite differing only by the direction of transport fluxes, the molecular mechanisms of translocation adopted by antiporters and symporters seem to be drastically different. We present chemical-kinetic models to quantitatively investigate this phenomenon. Our theoretical approach allows us to explain why antiporters mostly utilize a single-site transportation when only one molecule of any type might be associated with the channel. At the same time, the transport in symporters requires two molecules of different types to be simultaneously associated with the channel. In addition, we investigate the kinetic constraints and efficiency of symporters and compare them with the same properties of antiporters. Our theoretical analysis clarifies some important physical–chemical features of cellular trans-membrane transport.

Published under an exclusive license by AIP Publishing. https://doi.org/10.1063/5.0082589

I. INTRODUCTION

Biological cells are fundamental unit blocks of all living systems. They can be viewed as membrane-protected compartments where most relevant biochemical and biophysical processes are taking place.[1,2] Biological cells, however, cannot function in isolation, and efficient trans-membrane transport is required for their survival since nutrients must be moved in, while waste materials must be moved out.[1–5] While some small-size molecules might travel unaided across the semi-permeable cell membrane, most biologically important larger-size compounds must use specific channel proteins that allow them to pass cellular boundaries. It is also often necessary for some molecules to be moved against their concentration gradients across the cell membrane, and this action cannot be done without the input of energy.

Cellular transport adopted two different strategies for active translocation of materials. In the first one, known as primary active transport, the energy typically comes from the hydrolysis of ATP (adenosine triphosphate), a widely available source of energy in living cells.[1–3,6,7] The other approach, known as secondary active transport or cotransport, is more elegant and efficient from the cellular point of view. It explores the existing trans-membrane gradients for different compounds. The translocation of the molecule along its gradient would provide a source of free energy that might be used to move other species against their gradients. Secondary transporters couple the motion of the driving and the driven species, allowing

Published under an exclusive license by AIP Publishing

for the trans-membrane transport to occur.[3,6,8] The mechanisms of cotransport in biological cells have been intensively investigated in recent decades using a variety of experimental, theoretical, and computational methods. While significant advances have been already made, many aspects of these complex processes still remain not well understood.[9–14]

The protein channels responsible for secondary active transport are divided into two groups depending on the directions of the fluxes of the two types of molecules. If the directions of the driving and the driven molecules coincide, such transporters are labeled symporters.[6,15,16] However, if the molecular fluxes of the driving and the driven species occur in opposite directions, this corresponds to protein channels that are labeled antiporters.[17–19] Based on multiple experimental observations, it is widely believed that molecular translocations in both antiporters and symporters are a result of structural conformational changes taking place after the molecules bind the protein channels. These conformational transitions alternatively expose the transporters to only the outside or only the inside cellular regions, allowing for the transport to happen and for the channel to reset.[9–11,20,21] This view has strong structural and kinetic experimental support.[18,22–24]

Although both symporters and antiporters follow similar translocation mechanisms involving conformational changes exposing the compounds to opposite sides of the membrane and share many structural features,[6,24–26] surprisingly, the microscopic implementations of this mechanism for secondary transporters seem to be highly different. Experimental studies indicate that a large majority of antiporters utilize a so-called single-site alternating-access mechanism, where the transporter can only associate with one compound at a time.[6,27,28] The binding of any type of molecule with the transporter catalyzes conformational transitions that switch the orientation of the channel. The situation is very different for symporters where only a so-called two-site mechanism is realized. The simultaneous association of both driving and driven molecules with the protein channel leads to the conformational transitions, permitting the molecular transport.[16,29,30] It should also be mentioned that there are very few examples when the antiporters also utilize two simultaneous molecular associations with the channel,[23] but there are no exceptions, to the best of our knowledge, for symporters to use a single-site translocation mechanism.

These surprising experimental observations raised several important questions on the mechanisms of secondary active transport. Why do transporters that differ only in the direction of stimulated molecular fluxes exhibit such drastically different molecular mechanisms? What is the physical–chemical origin of this phenomenon? How does one quantify these observations? In addition, given that the latest theoretical study indicated that kinetics, and not thermodynamics, govern the functioning of antiporters,[14] the question is how this will change for the symporters. To answer these questions, we develop a chemical-kinetic approach that allows us to explicitly evaluate the transport dynamics of the single-site and the two-site translocation models. It is shown that the single-site model can only support the antiporters' activities, while the two-site models can be explored by both symporters and antiporters, although for structurally different protein channels. Furthermore, our theoretical analysis quantifies the efficiency and kinetic constraints of symporters, and the differences with antiporters are discussed.

II. CHEMICAL-KINETIC MODELS OF SECONDARY ACTIVE MEMBRANE TRANSPORT

Let us consider molecular translocations across secondary active transporters, as schematically shown in Fig. 1. We have two types of molecules, A and B, with concentrations c_A and c_B outside the cell (above the membrane in Fig. 1) and c_A' and c_B' inside the cell (below the membrane in Fig. 1), respectively. For convenience, we assume that molecules A are the driving species that move down along their trans-membrane gradient (from the outside region to inside region), defined via a parameter $g_A = c_A/c_A' > 1$, i.e., the concentration of the molecules A above the channel is always larger than the concentration of the molecules A below the channel ($c_A > c_A'$); see Fig. 1. The down-gradient motion of the molecules A supports the translocation of molecules B against their gradient. Two different situations can be realized as one can see from Fig. 1. If there are more B molecules below the channel ($c_B < c_B'$, $g_B = c_B/c_B' < 1$), then this corresponds to symporters, while for antiporters, we have more B molecules above the channel ($c_B > c_B'$, $g_B = c_B/c_B' > 1$). For transport to occur, a minimal energetic requirement is $g_A > g_B$ for antiporters and $g_A > 1/g_B$ for symporters.

Based on experimental observations and previous theoretical analysis, we propose several chemical-kinetic models to analyze the translocation dynamics in secondary active transport.[6,10,11,14] They are presented in Fig. 2. Each model postulates the existence of six chemical states of the protein channel depending on its occupation and direction of open conformations. This is because when the channel is facing up, it should have at least three different states: an empty channel, a channel occupied by one particle, and a channel occupied by another or both particles (see Fig. 2). Then, three similar "mirror-image" states should be added to the model when the channel is facing down. This picture clearly presents a minimal theoretical description since many more chemical states are involved in

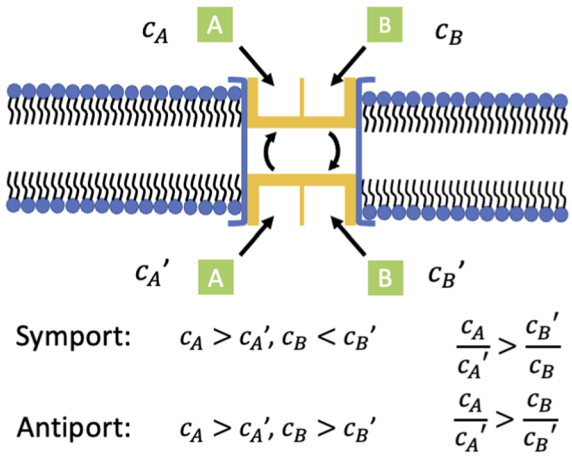

FIG. 1. A schematic view of the secondary active transport. Two types of molecules, *A* and *B*, translocate across the cellular membrane with intermediate binding inside the channel, stimulating the conformational change of the channel direction. Molecules *A* are considered to be the drivers of the motion of molecules *B*. Molecules *A* preferentially move from the upper part to the lower part. In symporters, molecules *B* also preferentially move in the same direction, while in antiporters, *B* translocates in the opposite direction.

Published under an exclusive license by AIP Publishing

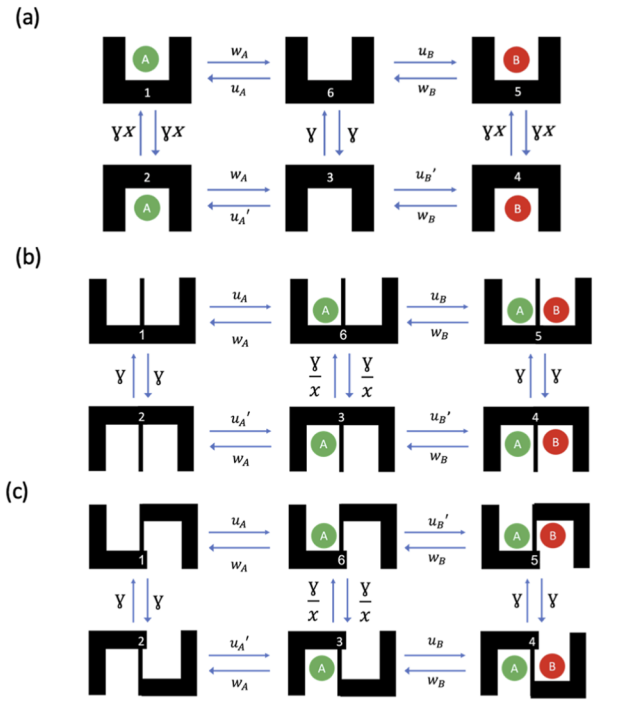

FIG. 2. Chemical-kinetic models of secondary active membrane transport. (a) A single-site alternating-access model for antiporters, (b) a double-site model for symporters, and (c) a double-site model for antiporters.

these complex transport processes. However, it is believed that such a theoretical approach should properly describe the main physics of the translocation dynamics via transporters since it accounts for the most relevant chemical states.[14]

The model presented in Fig. 2(a) reflects a single-site alternating-access mechanism of cotransport.[14] There are three states (1, 6, and 5) that have the channel open to the outside, while three other states (2, 3, and 4) correspond to the channel being open to the inside of the cell. The reversible binding of the molecules A from the outside is given by transitions $6 \leftrightarrow 1$, which happen with rates $u_A = kc_A$ and w_A, respectively. Similarly, the reversible association of the molecules B from outside is given by transitions $6 \leftrightarrow 5$ with rates $u_B = kc_B$ and w_B, respectively. The molecules A and B can also reversibly bind when the channel is facing the inside of the cell [Fig. 2(a)]. These chemical transitions are described by $3 \leftrightarrow 2$ with rates $u'_A = kc'_A$ and w'_A and by $3 \leftrightarrow 4$ with rates $u'_B = kc'_B$ and w'_B. For convenience, we assume that all dissociation rates of the same type of molecules are equal to each independently of the structural conformation of the transporter, i.e., $w_A = w'_A$ and $w_B = w'_B$. The structural inversion of the empty channel is described by transitions $6 \leftrightarrow 3$ with rates γ. At the same time, binding of the molecule A or B to the channel catalytically accelerates such transitions. These transition rates are given by γx where a dimensionless parameter x quantifies the catalytic effect of accelerated structural transition.[14] It has been argued that this chemical-kinetic model provides a reasonable description of the translocation dynamics in antiporters.[14] This means that while the flux of the molecules A is downward, it allows the molecules B to be transported from the inside to the outside of the cell against their gradient (recall that $c_B > c'_B$).

The chemical-kinetic model in Fig. 2(b) describes more complex two-site mechanisms of secondary transport. The channel has two sites where the substrates can bind, but first, only the molecule A can enter the empty channel facing up or facing down (transitions $1 \to 6$ and $2 \to 3$) with rates u_A and u'_A, respectively. The dissociations of the molecule A (transitions $6 \to 1$ and $3 \to 2$) are taking place with the rate w_A for both situations. The molecule B can reversibly associate to the channel only when the molecule A is already present in the channel [see Fig. 2(b)]. Microscopically, it means that binding of the molecule A modifies the structure of the channel, allowing the molecule B to enter. This corresponds to transitions $6 \leftrightarrow 5$ with the rates u_B and w_B and to transitions $3 \leftrightarrow 4$ with the rates u'_B and $w'_B = w_B$. When the channel is empty or doubly occupied, the structural conformational changes ($1 \leftrightarrow 2$ and $5 \leftrightarrow 4$) are taking place reasonably fast with the rates γ for both situations. However, as shown in Fig. 2(b), the presence of only one compound in the channel slows down such transitions ($6 \leftrightarrow 3$), and they happen with the rate γ/x. The dimensionless parameter x here quantifies the effect of inhibition of structural transition. This is the model for trans-membrane transportation by symporters.[6]

The chemical-kinetic model in Fig. 2(c) also describes the two-site translocation mechanism, but it corresponds to a different structural arrangement of the channel. The difference between the two-site models is that for the system in Fig. 2(b), both binding sites are simultaneously open to the outside or to the inside of the cell. For the system in Fig. 2(c), however, both sites are facing different sides of the membrane (one to the outside and one to the inside), and the structural transitions alternate their orientations. It has been argued that such a model might work for some antiporters, although the great majority of antiporters apparently follow a simpler single-site alternating-access model [Fig. 2(a)].[6,23]

It is important to note also that we consider the simplest models with two-site binding in which the molecule A binds first to the channel and it is released the last after the channel switches the conformations; see Figs. 2(b) and 2(c). One could also propose a situation when the molecule B binds first and released last after the conformational change. We checked (the results are not shown) that both models produce very similar results and follow essentially the same physics. For convenience, we utilize only one of those models presented in Figs. 2(b) and 2(c) in our theoretical calculations. One could also note the possibility of a mechanism in which two different conformations of the transporter exhibit different affinities to compounds A and B that might lead to a different order of binding and unbinding events in the system.

Note that in all three chemical-kinetic models in Fig. 2, we implicitly assumed that the free energies of the corresponding conformations facing up or facing down are the same. This is because there are no indications from both experimental and computational studies that the stability of the transporter is significantly impacted by conformational changes. This leads to identical transition rates for vertical transitions between states. It is expected that this should not affect the main physics of the translocation via symporters and antiporters much.

The main question that we are trying to answer is why antiporters mostly follow the single-site mechanisms while for

Published under an exclusive license by AIP Publishing

symporters only the two-site mechanism can be realized. For this purpose, we need to compare the dynamic properties of different chemical-kinetic models from Fig. 2. This can be done by defining a vector of probabilities to be found in different chemical states, $\mathbf{P} = \{P_1(t), P_2(t), P_3(t), P_4(t), P_5(t), P_6(t)\}$, where $P_j(t)$ $(j = 1, 2, \ldots, 6)$ is the probability to find the system in the state j at time t. The dynamics of the system is governed by the set of master equations that can be compactly written as a matrix expression,

$$\frac{d\mathbf{P}}{dt} = \mathbf{TP}, \tag{1}$$

where $\mathbf{T}$ is a transition rate matrix for each system. This means that the T_{ij} element of the matrix is given by the transition rate from the state i to the state j, while $T_{ii} = -\sum_{j=1}^{6} T_{ji}$. In addition, there is a normalization condition,

$$\sum_{j=1}^{6} P_j(t) = 1. \tag{2}$$

We are interested in large-time dynamics when the system reaches a stationary state and $\frac{d\mathbf{P}}{dt} = 0$. In this case, the set of master equations simplifies into a system of algebraic equations that can be solved exactly, as, for example, was already shown for the single-site alternating-access model [Fig. 2(a)].[14] This leads to explicit expressions for stationary probabilities of different chemical states. Similar calculations of dynamic properties can also be done for the two-site kinetic models [Figs. 2(b) and 2(c)]. In the supplementary material, we also present the explicit expressions for stationary probabilities for two-site chemical-kinetic models.

To analyze the differences in dynamic properties, we determine the stationary particle fluxes for the molecules A, J_A, and the molecules B, J_B. For the single-site alternating-access model, these fluxes are given by [see Fig. 2(a)]

$$J_A = \gamma x(P_1 - P_2), \quad J_B = \gamma x(P_4 - P_5). \tag{3}$$

These definitions assume that the flux of the molecules A is positive when the molecules A mostly translocate from the upper region to the lower region, and the particle current J_B is positive when the molecules B mostly move in the opposite direction; see Fig. 2(a).

For the two-site kinetic models, the expression for the particle fluxes is more complex. The molecular flux of the molecules A for both systems shown in Figs. 2(b) and 2(c) can be written as

$$J_A = \frac{\gamma}{x}(P_6 - P_3) + \gamma(P_5 - P_4). \tag{4}$$

This expression reflects the fact that the translocation of the molecule A can happen via two different paths ($6 \leftrightarrow 3$ and $5 \leftrightarrow 4$). Again, the positive flux is when the molecules A are transported from the upper side to the lower side. For the molecular flux of the particles B, we have

$$J_B = \pm\gamma(P_5 - P_4), \tag{5}$$

where "+" corresponds to the model in Fig. 2(b) and "−" corresponds to the model in Fig. 2(c). These expressions account for a single path for the translocation of B $(5 \leftrightarrow 4)$. For the model in Fig. 2(b), $J_B > 0$ when the flux is from the upper part to the lower part, and for the model in Fig. 2(c), the convention is opposite.

To quantify the efficiency of the secondary active transport, it is convenient to introduce a dimensionless parameter η,[14]

$$\eta = \frac{J_B}{J_A}. \tag{6}$$

It specifies how many molecules of type B might be driven by the translocation of one molecule A. In ideal situation of perfect secondary active transport, one could expect $\eta = 1$, but due to the realistic so-called "leakage" transitions, the efficiency is always less than one.[31] At the same time, this parameter quantitatively describes the performance of these protein channels.

III. RESULTS

Let us start with the single-site alternating-access model presented in Fig. 2(a). We would like to understand what kind of secondary transporters can be supported by this kinetic scheme. It was shown before that antiporters can function under this model for the following condition, obtained by enforcing $J_B < 0$:[14]

$$\frac{g_A}{g_B} > \frac{1 + \frac{2\gamma}{u'_A} + \frac{w_A}{xu'_A}}{1 + \frac{2\gamma}{u_A} + \frac{w_A}{xu_A}}. \tag{7}$$

This means that $g_A > 1$ $(c_A > c'_A)$ and $g_B > 1$ $(c_B > c'_B)$, but still, the molecules B can be moved from the inside region with lower concentration to the outside region with higher concentration.

One can check if symporters might also follow the same kinetic model. This can only happen in the parameter space outside of the region for antiporters, leading to the following condition:

$$\frac{g_A}{g_B} < \frac{1 + \frac{2\gamma}{u'_A} + \frac{w_A}{xu'_A}}{1 + \frac{2\gamma}{u_A} + \frac{w_A}{xu_A}} = g_A \frac{xu'_A + 2\gamma x + w_A}{xu_A + 2\gamma x + w_A}. \tag{8}$$

Similarly to antiporters, this criterion is derived by enforcing the flux of the compound B against its concentration gradient, or $J_B > 0$. However, because we assume that the molecules A are the drivers of the transport, i.e., $u_A > u'_A$, this inequality immediately leads to the conclusion that it can be satisfied only when $g_B > 1$. However, this contradicts with the condition for the symporter to function properly: c_B must be smaller than c'_B or g_B must be less than one. These arguments show that the single-site alternating-access model that works for antiporters can never be a correct model for symporters.

These surprising observations can be explained by analyzing the chemical-kinetic scheme in Fig. 2(a). For symporters, the molecules B must be moved following the pathway $6 \to 5 \to 4 \to 3$. However, there are two other processes that prevent this from happening. First, because the molecules A are the driving species, their association with the empty channel state facing up (state 6) is more probable, preventing the molecules B from binding to the channel. Second, the empty channel state facing down (state 3) does not have the same competition from the molecules A. On the contrary, since there are many molecules B inside the cell, the most probable sequence of events will be transitions $3 \to 4 \to 5 \to 6$, reversing any symport transport. These two factors effectively eliminate the possibility of symporters to utilize the single-site alternating-access mechanism of transportation.

Published under an exclusive license by AIP Publishing

Let us now consider the two-site chemical-kinetic model, as shown in Fig. 2(b). From the stationary probabilities of different states (explicitly given in the supplementary material), we can evaluate the particle fluxes using Eqs. (4) and (5). The symporter is realized when $J_B > 0$, and it can be shown that this happens when

$$\left(g_A - \frac{1}{g_B}\right) w_A x > \left(\frac{1}{g_B} - 1\right)\left[\gamma + g_A(\gamma + u'_A)\right]. \tag{9}$$

The symport transport is characterized by $g_A > 1$, $g_B < 1$ $(1/g_B > 1)$, and $g_A > 1/g_B$, which corresponds to the thermodynamic condition that there is enough energy provided by the molecules A translocating along their gradient to move the molecules B against their gradient. Equation (9) shows that symporters can only operate under additional conditions on their concentration gradients that arise due to specific kinetic mechanisms.

For antiporters to function, the condition must be reversed, leading to

$$\left(g_A - \frac{1}{g_B}\right) w_A x < \left(\frac{1}{g_B} - 1\right)\left[\gamma + g_A(\gamma + u'_A)\right]. \tag{10}$$

However, one of the properties of the antiport transport is $g_B > 1$ $(1/g_B < 1)$ since the molecules B have to translocate in the direction opposite to the molecules A. While the left-hand side of Eq. (10) is always positive, the right-hand side is always negative $(1/g_B - 1 < 0)$, and the inequality cannot be satisfied at any set of parameters. These arguments show that the antiporters cannot be realized in the two-site chemical-kinetic model from Fig. 2(b), while the symporters can function under these conditions.

Analyzing the chemical-kinetic scheme of the two-site translocation mechanism [Fig. 2(b)], one can easily understand why only the symport transport can be realized. In this case, the molecules B must preferentially move down (via the $5 \to 4$ path). This is accomplished by the fact that most of the transport of the driving molecules A also takes place in this transition. Because the parameter x is typically large, the translocations via the path $6 \to 3$ is minimal. However, for the antiporters to function, the molecules B must move up via the transition $4 \to 5$, which is less probable due to large driving by the molecules A in the opposite direction.

These theoretical arguments, however, also suggest that the antiport transport might follow the two-site chemical-kinetic mechanism if the binding sites for the molecules A and B face different sides of the membrane, as presented in Fig. 2(c). In this case, the driving of the molecules A via the transition $5 \to 4$ would also move the molecules B from the inside of the cell to the outside of the cell region. The conditions for the antiporters to function using this mechanism can be written as

$$(g_A - g_B) w_A x > (g_B - 1)\left[\gamma + g_A(\gamma + u'_A)\right]. \tag{11}$$

At the same time, the conditions for the symporters to utilize the model from Fig. 2(c), given by

$$(g_A - g_B) w_A x < (g_B - 1)\left[\gamma + g_A(\gamma + u'_A)\right], \tag{12}$$

cannot be realized because in this case, we have $g_B < 1$, and the right-hand side of the inequality will be negative, while the left-hand side is always positive. Then, no parameters can satisfy this condition.

Thus, our theoretical arguments indicate that symporters cannot explore the single-site alternating-access mechanism [Fig. 2(a)], and this agrees well with the available experimental observations.[6] However, they can follow the two-site kinetic models when two sites are simultaneously facing the same direction [Fig. 2(b)]. At the same time, theoretical calculations indicate that antiporters might utilize both the single-site alternating-access model [Fig. 2(a)] and the two-site model with the binding sites facing different sides of the membrane [Fig. 2(c)]. These theoretical results also suggest that the specific microscopic realization of the translocation mechanism in cotransport depends on the topology of the underlying chemical-kinetic scheme and on the directions of the molecular fluxes of species involved in the transport. Our theoretical approach can also be used to compare two different possible translocation mechanisms for antiporters since the dynamic properties can be explicitly evaluated.

The results of our calculations are presented in Fig. 3 where the fluxes of the molecules B and the efficiency of the antiporters are estimated for different ranges of parameters and for different translocation models. Increasing the gradient of the molecules B decreases the driven flux because of the diminishing driving force, which qualitatively correlates with the quantity $g_A - g_B$; see Fig. 3(a). The single-site model produces higher flux for relatively small g_B, while for larger g_B, the two-site model becomes more productive.

Interestingly, changing the dissociation rate w_A has a very different effect on the fluxes of the molecules B in the single-site and two-site models, as shown in Fig. 3(b). Increasing w_A lowers the flux in the single-site mechanism, while it simultaneously increases the flux in the two-site mechanism. This can be understood by analyzing the corresponding chemical-kinetic schemes in Figs. 2(a) and 2(b). Increasing the dissociation rate w_A in the single-site model slows down the translocation of the molecules A across the channel

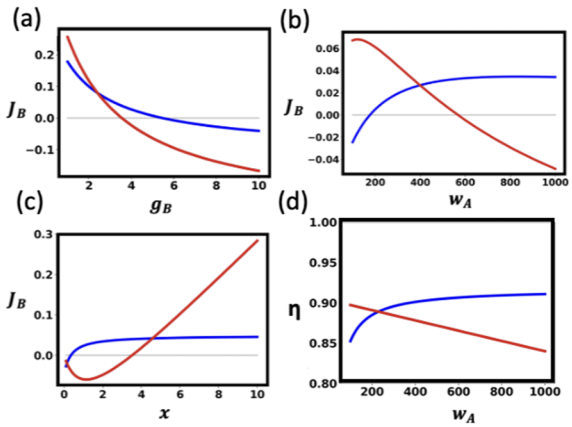

FIG. 3. Comparisons of dynamic properties of antiporters in the single-site model (red curves) and in the two-site model (blue curves). (a) The molecular flux J_B as a function of the gradient parameter $g_B = c_B/c'_B$. (b) The molecular flux J_B as a function of the dissociation rate w_A. (c) The molecular flux J_B as a function of the catalytic/inhibition parameter x. (d) The efficiency $\eta = j_B/J_A$ as a function of the dissociation rate w_A. The following parameters were used in calculations: $w_B = 500$, $g_A = 10$, and $x = 2$ in (c) and $x = 50$ in (d).

Published under an exclusive license by AIP Publishing

$(1 \rightarrow 6)$, which is the driving force for the antiporter. For the two-site model, increasing the rate w_A resets the system faster (transition $3 \rightarrow 1$) and it prevents the molecules B from binding the channel in state 3.

It is also interesting to consider the effect of the catalytic/inhibition parameter x on the molecular fluxes J_B, as presented in Fig. 3(c). In the regime where antiporters function $(J_B > 0)$, increasing x also leads to larger fluxes. However, the effect is much stronger for the single-site model than for the two-site model. The reason for this is that in the alternating-access mechanism [Fig. 2(a)], varying x affects two transitions, $1 \leftrightarrow 2$ and $5 \leftrightarrow 4$, while in the two-site mechanism [Fig. 2(c)], the inhibition parameter only modifies one "leaking" transition $6 \leftrightarrow 3$.

The efficiencies of the antiporters also differ significantly in the single-site and the two-site model, as shown in Fig. 3(d). Increasing the dissociation rate w_A lowers the efficiency in the single-site mechanism and increases the efficiency in the two-site model. This is a consequence of how the variation in the same dissociation rate influences the molecular flux J_B, as shown in Fig. 3(b), since $\eta = J_B/J_A$.

One could also note that biologically relevant parameters correspond to relatively large values of the catalytic/inhibition parameter x, relatively small concentration gradients g_B, and not too large dissociation rates w_A. However, at these conditions, the single-site alternating-access model seems to be more efficient, and this might be the reason why this mechanism is preferably chosen in nature for antiporters.

Our recent theoretical study of antiporters that investigated in detail the single-site alternating-access mechanism indicated that kinetics, rather than thermodynamics, determine the functioning of these protein channels.[14] It was also argued that this is a consequence of the presence of "leaking" transition [$6 \leftrightarrow 3$ in Fig. 2(a)] that requires additional energy to be compensated. It is interesting to investigate if kinetics or thermodynamics specify the operating rules for symporters that follow the two-site mechanism [Fig. 2(b)]. From Eq. (9), we obtain the following condition for the symporters to be functional:

$$\frac{1}{g_B} < \frac{g_A(w_A x + \gamma + u'_A) + \gamma}{g_A(\gamma + u'_A) + \gamma + w_A x}. \tag{13}$$

Figure 4 shows the parameter space where symporters operate, and one can see that, similarly to antiporters, the kinetics govern their activities and not thermodynamics. Again, this is the consequence of the presence of "leaking" transition [$6 \leftrightarrow 3$ in Fig. 2(b)]. Increasing the inhibition effect (large x) should bring the symporters closer to the thermodynamic limit, $1/g_B < g_A$, and one can check that this can be obtained from Eq. (13). However, there is a difference with the analogous behavior for antiporters. For very large values of the gradient of the molecules A $(g_A \gg 1)$, there is a saturation effect and Eq. (13) changes into

$$\frac{1}{g_B} < 1 + \frac{w_A x}{\gamma + u'_A}. \tag{14}$$

This means that the further increase in the driving force (larger g_A) will not improve the efficiency of symporters. This can be understood if we compare the chemical-kinetic schemes for the single-site and two-site translocation mechanisms [Figs. 2(a) and 2(b)]. While

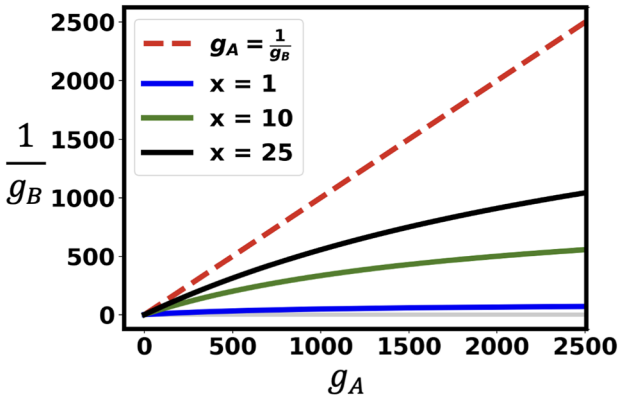

FIG. 4. Comparison of thermodynamic and kinetic conditions for functioning of symporters. The red dashed line describes the thermodynamic boundary, while the solid lines correspond to kinetic boundaries for different inhibition parameter x. The following parameters were used in calculations: $u_A = 1000\ s^{-1}$, $u'_B = 1000\ s^{-1}$, $w_A = 100\ s^{-1}$, and $w_B = 100\ s^{-1}$.

in the alternating-access mechanism there is only one path for moving the molecule A across the membrane $(1 \leftrightarrow 2)$, there are two such transitions in the two-site mechanism ($6 \leftrightarrow 3$ and $5 \leftrightarrow 4$). Increasing g_A while keeping all other parameters fixed will significantly increase the leakage current, and this does not allow for the efficiency of the symporters to be improved.

Using our theoretical approach, we can also investigate the efficiency of symporters as translocating machines. One can define $g_A g_B$ as an effective driving force for translocation because the transport in these channels can only happen for $g_A > 1/g_B$. In Fig. 5, we evaluate the efficiency of symporters as a function of such driving force

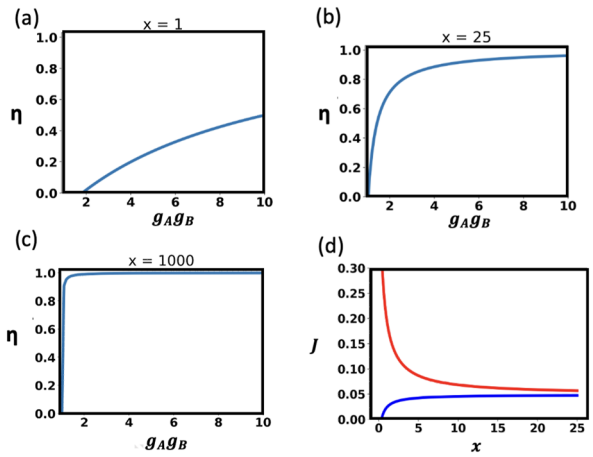

FIG. 5. Efficiency as a function of the product of the two concentration gradients at (a) $x = 1$, (b) $x = 25$, and (c) $x = 1000$. (d) The flow rate of compounds A (red) and B (blue) getting closer together as x increases. The following parameters were used in calculations: $\gamma = 1$, $u_A = 1000$, $u'_B = 1000$, $u'_A = 100$, $w_A = 1000$, and $w_B = 1000$. In (d), $u_B = 300$.

Published under an exclusive license by AIP Publishing

for different values of the inhibition parameter x. Increasing the inhibition (larger x) always makes symporters more efficient as we increase the driving force. However, for small x, the effect is quite moderate [Fig. 5(a)], while for large x, even a relatively weak driving immediately leads to the efficiency $\eta \simeq 1$ [Fig. 5(c)]. This result also shows the robustness of symporters to external fluctuations for large inhibition parameters x. For large values of x, the current through the leakage transition decreases almost to zero, lowering the effect of the transition that is the main source of inefficiency in the system. As one can also see, the fluctuations in the concentrations of driving molecules A (which would lead to changing $g_A g_B$) will not influence the efficiency of the transport for large values of x much.

IV. SUMMARY AND CONCLUSIONS

In this paper, we theoretically investigated the molecular mechanisms of secondary active transport by protein membrane channels. It is accomplished by explicitly calculating the stationary properties of several chemical-kinetic models of translocation. Our theoretical analysis shows that the topology of underlying kinetic schemes and the direction of molecular fluxes determine the specific molecular realizations of the transport. This allows us to explain why antiporters mostly follow the single-site alternating-access mechanism, while symporters cannot utilize this method of transport. At the same time, symporters can only follow the specific two-site translocation mechanism, which is not possible for antiporters. Our theoretical calculations explain the surprising experimental observations on different translocation mechanisms for two main types of secondary membrane transporters. In addition, it is shown that, similarly to antiporters, kinetics determine the operating rules for symporters. Physical–chemical arguments to explain this result are provided. Furthermore, the efficiency of symporters as translocating machines is explicitly evaluated. It is argued that at realistic cellular conditions, the robust transportation is expected for these channels.

Although our theoretical approach provides a simple, intuitive, and thermodynamically consistent picture of membrane transport, it is important to discuss its limitations. In our analysis, we assumed the same dissociation rates for substrates on both sides of the membrane, while in real systems, this might not be the case. Additionally, we implicitly assumed in the two-site models that the inhibitory effect of the binding of one molecule is fully canceled by the binding of the other, when the true effect of the second molecule association might not be so simple. In addition, the free energies of corresponding channel conformations facing up and facing down are taken to be the same, but this also requires careful investigation. Probably, more importantly, our analysis did not consider many other chemical states in the system. Although our choice of the most relevant chemical states seems to be reasonable, more advanced calculations and experimental measurements are needed to test it. Finally, it will also be interesting to investigate the role of stoichiometry in the membrane transport. It is known that in many symporters and antiporters, the ratio of associating molecules A and B frequently deviates from 1 : 1 assumed in this work. Whether this is dictated by energetic requirements or if there are other reasons that might help to optimize the cotransport phenomena is a question that remains to be answered.

SUPPLEMENTARY MATERIAL

See the supplementary material for results of calculations for stationary probabilities of two-site models for antiporters and symporters.

ACKNOWLEDGMENTS

We acknowledge the support from the Welch Foundation (Grant No. C-1559), from the NSF (Grant Nos. CHE-1953453 and MCB-1941106), and from the Center for Theoretical Biological Physics sponsored by the NSF (Grant No. PHY-2019745).

AUTHOR DECLARATIONS

Conflict of Interest

The authors have no conflicts to disclose.

DATA AVAILABILITY

The data that support the findings of this study are available from the corresponding author upon reasonable request.

REFERENCES

[1] B. Alberts, A. Johnson, J. Lewis, D. Morgan, M. Raff, K. Roberts, and P. Walter, *Molecular Biology of the Cell*, 6th ed. (Garland Science, New York, 2014).
[2] H. Lodish, A. Berk, C. A. Kaiser, C. Kaiser, M. Krieger, M. P. Scott, A. Bretscher, H. Ploegh, P. Matsudaira, *et al.*, *Molecular Cell Biology* (Macmillan, 2008).
[3] W. Stillwell, *An Introduction to Biological Membranes: Composition, Structure and Function* (Elsevier, 2016).
[4] S. Faham, A. Watanabe, G. M. Besserer, D. Cascio, A. Specht, B. A. Hirayama, E. M. Wright, and J. Abramson, "The crystal structure of a sodium galactose transporter reveals mechanistic insights into Na^+/sugar symport," Science **321**, 810–814 (2008).
[5] A. Schulz, D. Beyhl, I. Marten, A. Wormit, E. Neuhaus, G. Poschet, M. Büttner, S. Schneider, N. Sauer, and R. Hedrich, "Proton-driven sucrose symport and antiport are provided by the vacuolar transporters SUC4 and TMT1/2," Plant J. **68**, 129–136 (2011).
[6] M. V. LeVine, M. A. Cuendet, G. Khelashvili, and H. Weinstein, "Allosteric mechanisms of molecular machines at the membrane: Transport by sodium-coupled symporters," Chem. Rev. **116**, 6552–6587 (2016).
[7] K. Niinuma, Y. Kato, H. Suzuki, C. A. Tyson, V. Weizer, J. E. Dabbs, R. Froehlich, C. E. Green, and Y. Sugiyama, "Primary active transport of organic anions on bile canalicular membrane in humans," Am. J. Physiol.: Gastrointest. Liver Physiol. **276**, G1153–G1164 (1999).
[8] S. B. Poulsen, R. A. Fenton, and T. Rieg, "Sodium-glucose cotransport," Curr. Opin. Nephrol. Hypertens. **24**, 463 (2015).
[9] L. R. Forrest, R. Krämer, and C. Ziegler, "The structural basis of secondary active transport mechanisms," Biochim. Biophys. Acta, Bioenerg. **1807**, 167–188 (2011).
[10] O. Boudker and G. Verdon, "Structural perspectives on secondary active transporters," Trends Pharmacol. Sci. **31**, 418–426 (2010).
[11] Y. Shi, "Common folds and transport mechanisms of secondary active transporters," Annu. Rev. Biophys. **42**, 51–72 (2013).
[12] A. George, P. Bisignano, J. M. Rosenberg, M. Grabe, and D. M. Zuckerman, "A systems-biology approach to molecular machines: Exploration of alternative transporter mechanisms," PLoS Comput. Biol. **16**, e1007884 (2020).
[13] P. Bisignano, M. A. Lee, A. George, D. M. Zuckerman, M. Grabe, and J. M. Rosenberg, "A kinetic mechanism for enhanced selectivity of membrane transport," PLoS Comput. Biol. **16**, e1007789 (2020).
[14] A. Berlaga and A. B. Kolomeisky, "Molecular mechanisms of active transport in antiporters: Kinetic constraints and efficiency," J. Phys. Chem. Lett. **12**, 9588–9594 (2021).

Published under an exclusive license by AIP Publishing

[15]E. Darrouzet, S. Lindenthal, D. Marcellin, J.-L. Pellequer, and T. Pourcher, "The sodium/iodide symporter: State of the art of its molecular characterization," Biochim. Biophys. Acta, Biomembr. **1838**, 244–253 (2014).
[16]V. Navratna and E. Gouaux, "Insights into the mechanism and pharmacology of neurotransmitter sodium symporters," Curr. Opin. Struct. Biol. **54**, 161–170 (2019).
[17]E. Padan, M. Venturi, Y. Gerchman, and N. Dover, "Na^+/H^+ antiporters," Biochim. Biophys. Acta, Bioenerg. **1505**, 144–157 (2001).
[18]C. J. Law, P. C. Maloney, and D.-N. Wang, "Ins and outs of major facilitator superfamily antiporters," Annu. Rev. Microbiol. **62**, 289–305 (2008).
[19]M. Ito, M. Morino, and T. A. Krulwich, "Mrp antiporters have important roles in diverse bacteria and archaea," Front. Microbiol. **8**, 2325 (2017).
[20]S. Weyand, T. Shimamura, S. Yajima, S. Suzuki, O. Mirza, K. Krusong, E. P. Carpenter, N. G. Rutherford, J. M. Hadden, J. O'Reilly *et al.*, "Structure and molecular mechanism of a nucleobase–cation–symport-1 family transporter," Science **322**, 709–713 (2008).
[21]X. Gao, F. Lu, L. Zhou, S. Dang, L. Sun, X. Li, J. Wang, and Y. Shi, "Structure and mechanism of an amino acid antiporter," Science **324**, 1565–1568 (2009).
[22]C. J. Law, Q. Yang, C. Soudant, P. C. Maloney, and D.-N. Wang, "Kinetic evidence is consistent with the rocker-switch mechanism of membrane transport by GlpT," Biochemistry **46**, 12190–12197 (2007).
[23]R. K. Pradhan, D. A. Beard, and R. K. Dash, "A biophysically based mathematical model for the kinetics of mitochondrial Na^+-Ca^{2+} antiporter," Biophys. J. **98**, 218–230 (2010).
[24]D. Drew and O. Boudker, "Shared molecular mechanisms of membrane transporters," Annu. Rev. Biochem. **85**, 543–572 (2016).
[25]L. R. Forrest and G. Rudnick, "The rocking bundle: A mechanism for ion-coupled solute flux by symmetrical transporters," Physiology **24**, 377–386 (2009).
[26]J. Abramson, H. R. Kaback, and S. Iwata, "Structural comparison of lactose permease and the glycerol-3-phosphate antiporter: Members of the major facilitator superfamily," Curr. Opin. Struct. Biol. **14**, 413–419 (2004).
[27]D. W. Hilgemann and C.-C. Lu, "Gat1 (Gaba:Na^+:Cl^-) cotransport function: Database reconstruction with an alternating access model," J. Gen. Physiol. **114**, 459–476 (1999).
[28]L. R. Forrest, Y.-W. Zhang, M. T. Jacobs, J. Gesmonde, L. Xie, B. H. Honig, and G. Rudnick, "Mechanism for alternating access in neurotransmitter transporters," Proc. Natl. Acad. Sci. U. S. A. **105**, 10338–10343 (2008).
[29]S. Oh and O. Boudker, "Kinetic mechanism of coupled binding in sodium-aspartate symporter GltPh," eLife **7**, e37291 (2018).
[30]H. R. Kaback, "A chemiosmotic mechanism of symport," Proc. Natl. Acad. Sci. U. S. A. **112**, 1259–1264 (2015).
[31]T. L. Hill, *Free Energy Transduction and Biochemical Cycle Kinetics* (Courier Corporation, 2005).

Published under an exclusive license by AIP Publishing